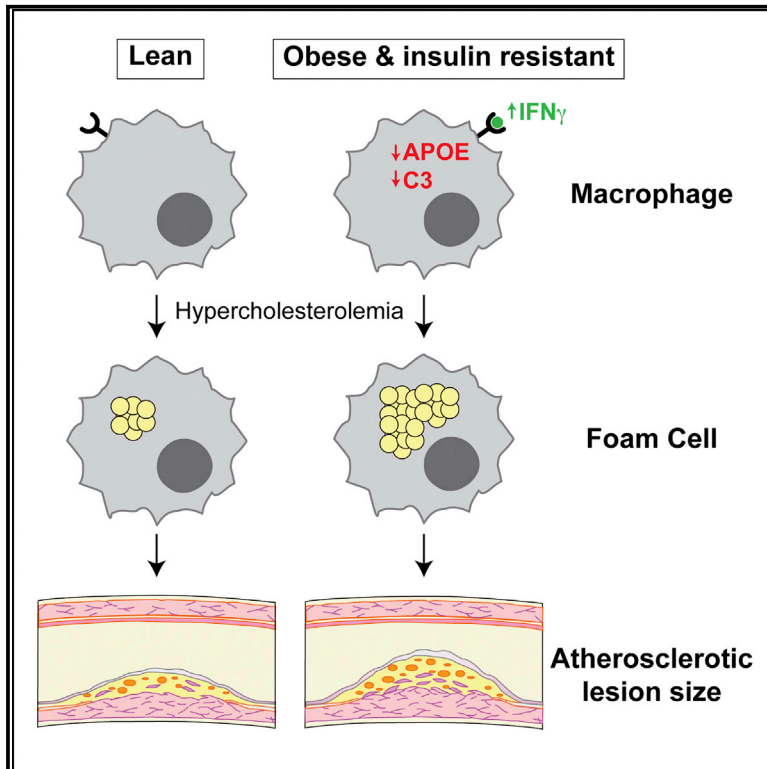Article

Obesity and Insulin Resistance Promote Atherosclerosis through an IFNγ-Regulated Macrophage Protein Network

Graphical Abstract

Authors

Catherine A. Reardon, Amulya Lingaraju, Kelly Q. Schoenfelt, ..., Howard Shuman, Tomas Vaisar, Lev Becker

Correspondence

levb@uchicago.edu

In Brief

Obesity and insulin resistance are major risk factors for cardiovascular disease, but the underlying mechanisms are poorly understood. Reardon et al. show that obesity and insulin resistance induce an IFNγ-macrophage pathway that exacerbates foam cell formation and aortic lesion size in atherosclerotic mice.

Highlights

- Obesity and insulin resistance induces IFNγ production by T cells

- IFNγ targets macrophage MSRN proteins and promotes foam cell formation

- Deleting myeloid cell *Ifngr1* attenuates atherosclerosis in obese/IR *Ldlr−/−* mice

- Deleting myeloid cell *Ifngr1* does not affect atherosclerosis in lean *Ldlr−/−* mice

CellPress

Article

Obesity and Insulin Resistance Promote Atherosclerosis through an IFNγ-Regulated Macrophage Protein Network

Catherine A. Reardon,[1,2,8] Amulya Lingaraju,[2,3,8] Kelly Q. Schoenfelt,[2] Guolin Zhou,[2] Chang Cui,[2] Hannah Jacobs-El,[2] Ilona Babenko,[4] Andrew Hoofnagle,[5] Daniel Czyz,[6] Howard Shuman,[6,7] Tomas Vaisar,[4] and Lev Becker[1,2,9,*]
[1]Committee on Molecular Metabolism and Nutrition, The University of Chicago, Chicago, IL 60637, USA
[2]Ben May Department for Cancer Research, The University of Chicago, Chicago, IL 60637, USA
[3]Committee on Molecular Pathogenesis and Molecular Medicine, The University of Chicago, Chicago, IL 60637, USA
[4]Department of Medicine, University of Washington, Seattle, WA 98195, USA
[5]Department of Laboratory Medicine, University of Washington, Seattle, WA 98195, USA
[6]Department of Microbiology, The University of Chicago, Chicago, IL 60637, USA
[7]Committe on Microbiology, The University of Chicago, Chicago, IL 60637, USA
[8]These authors contributed equally
[9]Lead Contact
*Correspondence: levb@uchicago.edu
https://doi.org/10.1016/j.celrep.2018.05.010

SUMMARY

Type 2 diabetes (T2D) is associated with increased risk for atherosclerosis; however, the mechanisms underlying this relationship are poorly understood. Macrophages, which are activated in T2D and causatively linked to atherogenesis, are an attractive mechanistic link. Here, we use proteomics to show that diet-induced obesity and insulin resistance (obesity/IR) modulate a pro-atherogenic "macrophage-sterol-responsive-network" (MSRN), which, in turn, predisposes macrophages to cholesterol accumulation. We identify IFNγ as the mediator of obesity/IR-induced MSRN dysregulation and increased macrophage cholesterol accumulation and show that obesity/IR primes T cells to increase IFNγ production. Accordingly, myeloid cell-specific deletion of the IFNγ receptor (Ifngr1−/−) restores MSRN proteins, attenuates macrophage cholesterol accumulation and atherogenesis, and uncouples the strong relationship between hyperinsulinemia and aortic root lesion size in hypercholesterolemic Ldlr−/− mice with obesity/IR, but does not affect these parameters in Ldlr−/− mice without obesity/IR. Collectively, our findings identify an IFNγ-macrophage pathway as a mechanistic link between obesity/IR and accelerated atherogenesis.

INTRODUCTION

Compared to non-diabetics, patients with type 2 diabetes (T2D) have a 4-fold increased risk for cardiovascular disease (CVD) during their lifetime, and have a greater overall plaque burden and higher rate of multi-vessel disease (Beckman et al., 2002;

Gore et al., 2015; Haffner et al., 1998; Hayward et al., 2015). Indeed, the 7-year incidence of first myocardial infarction (MI) or death in type 2 diabetics is ∼6-fold higher than in type 2 diabetics, and the 5-year mortality rate following an MI is nearly double for patients with T2D compared to non-diabetics.

Although patients with T2D face a significant risk for developing CVD, the mechanisms underlying this risk are poorly understood. In epidemiological studies, traditional risk factors, such as smoking, hypertension, low-density lipoprotein (LDL) cholesterol, high-density lipoprotein (HDL) cholesterol, total cholesterol, and triglyceride levels, do not explain the risk associated with CVD in type 2 diabetic patients (Beckman et al., 2002; Gore et al., 2015; Haffner et al., 1998; Hayward et al., 2015). Moreover, intervention studies showed that increased mortality is observed even when plasma cholesterol levels are aggressively lowered with statin treatment, hypertension is controlled, or with aggressive glycemic control (Banach et al., 2016; Gore et al., 2015).

Macrophages may represent an important cellular link between T2D and atherosclerosis. Macrophages are inappropriately activated during diet-induced obesity and insulin resistance (obesity/IR) (Chawla et al., 2011; Kratz et al., 2014; McNelis and Olefsky, 2014), and macrophages that accumulate excess cholesterol (foam cells) are causatively linked to initiation, progression, and rupture of atherosclerotic plaques (Li and Glass, 2002; Moore et al., 2013; Tabas and Bornfeldt, 2016). For example, their inability to clear cholesterol leads to the formation of foam cells, their defective clearance of apoptotic cells in the artery wall promotes necrotic core formation and increases plaque complexity, and their increased secretion of proteases destabilizes atherosclerotic plaques and promotes plaque vulnerability. Thus, the idea that obesity/IR alters macrophages in a way that promotes atherogenesis is an attractive hypothesis.

Although attractive, this hypothesis has been difficult to test experimentally because diets that promote obesity/IR in atherosclerotic mice also elevate plasma cholesterol levels. Thus, it has been challenging to distinguish macrophage pathways driven by
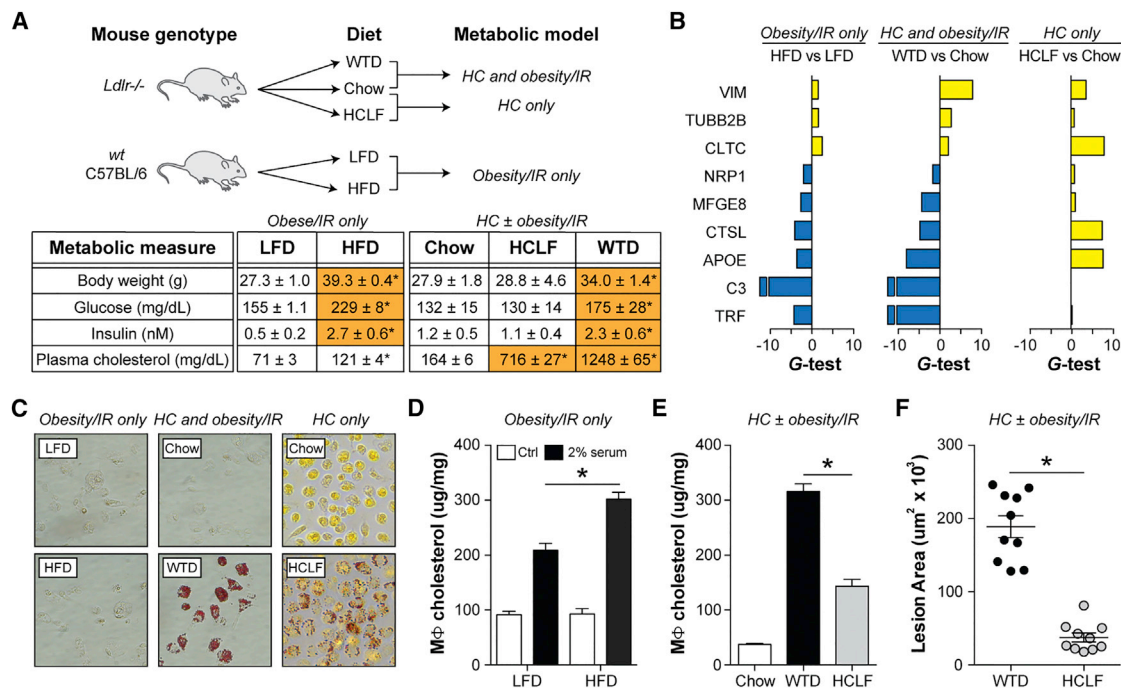
Figure 1. Obesity/IR Targets the MSRN, Promotes Macrophage Cholesterol Loading, and Exacerbates Atherosclerosis

(A–F) "Obesity/IR only" model: WT C57BL/6 mice were fed a low-fat diet (LFD) or high-fat diet (HFD) for 9 weeks. "HC ± obesity/IR" models: *Ldlr−/−* mice were fed a chow diet, a Western-type diet (WTD), or a high-cholesterol-low-fat (HCLF) diet for 12 weeks.

(A) Metabolic parameters.

(B) Proteomics analysis of peritoneal macrophages. Differentially abundant proteins (yellow, up; blue, down) were identified based on the *G*-test (*G* > 1.5) and t test (p < 0.05).

(C) Oil-red-O staining of peritoneal macrophages.

(D) Cholesterol levels in peritoneal macrophages treated with/without 2% serum from WTD-fed *Ldlr−/−* mice.

(E) Cholesterol levels in peritoneal macrophages.

(F) Aortic root lesion area.

Results are mean ± SEM. *p < 0.05 (t test). n = 5–10 mice/group. See also Figures S1 and S2 and Table S1.

hypercholesterolemia, from those controlled by the concomitant obesity/IR that develops when *Ldlr−/−* or *Apoe−/−* mice are fed the Western-type diet.

To overcome this problem, we combined genetic and dietary interventions to study macrophages in the presence of hypercholesterolemia and obesity/IR, alone or in combination. Using an unbiased proteomics approach, we identified an obesity/IR-driven interferon-gamma (IFNγ) pathway that targets the macrophage-sterol-responsive-network (MSRN) (Becker et al., 2010) to promote foam cell formation. We show that blocking this pathway in macrophages *in vivo* (by deleting *Ifngr1* in myeloid cells) normalized MSRN proteins and attenuated foam cell formation and atherosclerosis in *Ldlr−/−* mice with obesity/IR, but had no effect on these parameters in the absence of obesity/IR. Collectively, our studies identify an IFNγ-macrophage pathway as a mechanistic link between obesity/IR and accelerated atherogenesis.

RESULTS

Obesity/IR Targets the MSRN and Promotes Foam Cell Formation

To determine if obesity/insulin resistance (IR) alters macrophages to promote atherosclerosis, we used genetic models

and dietary interventions to study macrophages in mice with (1) "obesity/IR only," (2) "hypercholesterolemia (HC) and obesity/IR," and (3) "HC only" (Hartvigsen et al., 2007) (Figure 1A). This approach allowed us to test whether obesity/IR was sufficient to alter macrophages in normocholesterolemic mice and necessary to produce similar changes in hypercholesterolemic mice.

We used an unbiased proteomics approach to study how the various conditions affected protein abundance patterns in elicited peritoneal macrophages, whose responses to atherosclerosis modifying perturbations *in vivo* are reasonable surrogates for artery wall macrophages (Becker et al., 2010; Li et al., 2004).

We started with the "obesity/IR only" model, where C57BL/6 mice were fed a low-fat diet (LFD) or high-fat diet (HFD) for 9 weeks. Proteomic analyses of purified peritoneal macrophages (Figure S1) identified 27 secreted proteins that were altered by obesity/IR (false discovery rate [FDR] < 5%) (Figure S2). Nine of those proteins resided in a pro-atherogenic, MSRN (Figure 1B; Table S1) we previously identified in foam cells from hypercholesterolemic *Ldlr−/−* mice (Becker et al., 2010).

Although we previously identified the MSRN as a "sterol-responsive" protein network, MSRN protein changes in the
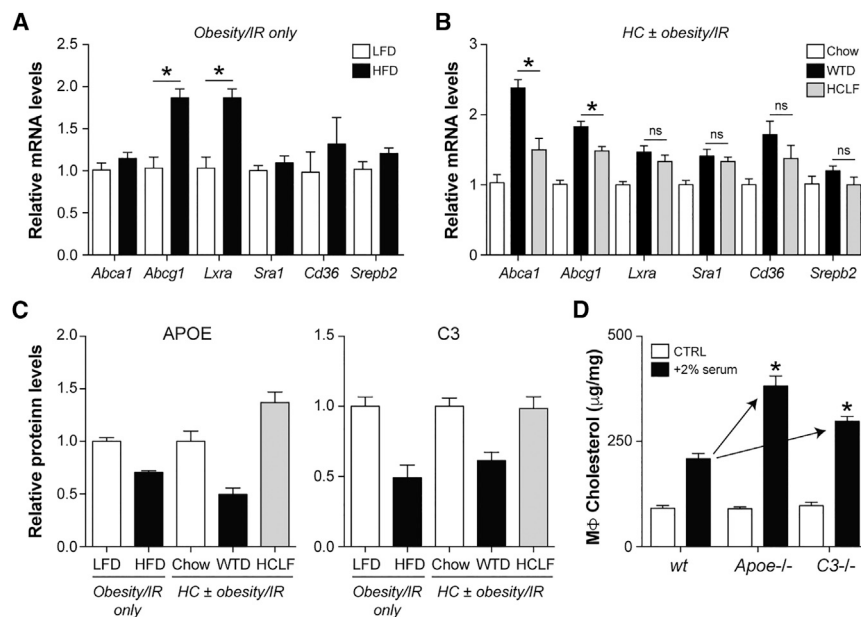
Figure 2. MSRN Protein Dysregulation Promotes Macrophage Foam Cell Formation

(A and B) Peritoneal macrophage mRNA levels for several genes involved in cholesterol metabolism in WT C57BL/6 mice fed a LFD or a HFD ("obesity/IR only" model, A) or in *Ldlr−/−* mice fed chow, a WTD, or a HCLF diet ("HC ± obesity/IR" models, B).

(C) Peritoneal macrophage media protein levels for APOE and C3.

(D) Peritoneal macrophages were isolated from 8-week-old WT, *Apoe−/−*, or *C3−/−* C57BL/6 mice fed a LFD. Macrophages were treated were with and without 2% serum from WTD-fed *Ldlr−/−* mice, and cholesterol levels were quantified. Results are mean ± SEM.

*p < 0.05 (t test). n = 5 mice/group.

"obesity/IR model only" occurred independent of changes in macrophage cholesterol or triglyceride levels (Figures 1C and S2), raising the possibility that a significant portion of this pro-atherogenic network was actually regulated by obesity/IR.

To test this, we asked whether eliminating obesity/IR could correct the 9 MSRN proteins in hypercholesterolemic *Ldlr−/−* mice. All 9 MSRN proteins were similarly dysregulated in the "HC and obesity/IR" model, but most were normalized or counter-regulated in the "HC only" model (Figure 1B; Table S1), even though macrophages were loaded with cholesterol (Figure 1C). For example, APOE levels were lowered in Western-type diet (WTD) fed *Ldlr−/−* mice but raised in high-cholesterol-low-fat (HCLF) diet-fed mice, findings that agree with the induction of APOE in macrophages loaded with cholesterol *in vitro* (Figure S2) (Basu et al., 1981).

APOE promotes reverse cholesterol efflux in macrophages, and its expression by macrophages restrains atherosclerosis (Fazio et al., 2002). The suppression of APOE by obesity/IR prompted us to determine whether obesity/IR promotes foam cell formation.

We first tested this in the "obesity/IR" only model. Since wild-type (WT) C57BL/6 mice fed the HFD have low plasma cholesterol levels we could not test this *in vivo*. Instead, we isolated peritoneal macrophages from these mice, exposed them to high levels of atherogenic lipoproteins (2% serum from WTD-fed *Ldlr−/−*), and found that obesity/IR induced by the HFD enhanced cholesterol accumulation (Figure 1D).

Next, we investigated whether eliminating obesity/IR from hypercholesterolemic mice ("HC ± obesity/IR" models) attenuated foam cell formation *in vivo*. Peritoneal macrophages from HCLF diet-fed *Ldlr−/−* mice had lower cholesterol levels than WTD-fed mice (Figure 1E). As previously described (Hartvigsen et al., 2007), aortic root lesion area was also lessened in HCLF diet-fed *Ldlr−/−* mice (Figure 1F). However, plasma cholesterol levels were lowered in HCLF diet-fed mice (see Figure 1A), high-lighting the problem of dissociating effects of obesity/IR and hypercholesterolemia. We overcame this by identifying the regulator of the MSRN, deleting it, and showing attenuation of macrophage cholesterol loading and atherosclerosis only in the presence of obesity/IR (see below).

MSRN Protein Dysregulation Promotes Macrophage Foam Cell Formation

Why did macrophages from obese/IR mice accumulate more cholesterol? One possibility is that this was due to defects in non-MSRN proteins involved in cholesterol metabolism. Arguing against this, mRNA levels of *Abca1*, *Abcg1*, *Lxra*, *Cd36*, *Sra1*, or *Srebp2* were unaffected or regulated to oppose cholesterol accumulation in all of the models tested (Figures 2A and 2B).

Increased cholesterol accumulation could also be due to altered MSRN proteins such as APOE and C3, which were lowered by obesity/IR in WT and *Ldlr−/−* mice (Figure 2C), and previously implicated in lipid metabolism (Barbu et al., 2015; Fazio et al., 2002). Peritoneal macrophages from lean 8-week-old *Apoe−/−* or *C3−/−* C57BL/6 mice accumulated more cholesterol (relative to WT) following exposure to 2% serum from WTD-fed *Ldlr−/−* mice (Figure 2D). Thus, obesity/IR may promote macrophage cholesterol accumulation by suppressing MSRN proteins such as APOE and C3.

IFNγ Targets MSRN Proteins *In Vitro* and *In Vivo*

Next, we sought to determine how obesity/IR alters MSRN proteins. We considered the possibility that hyperglycemia and/or hyperinsulinemia was responsible, but found that exposing peritoneal macrophages to high levels of glucose and insulin, individually or in combination, had no effect on APOE or MFGE8 (Figure 3A).

In addition to elevated glucose/insulin, patients with T2D also exhibit low-grade inflammation (Donath and Shoelson, 2011). We tested various cytokines for their ability to target MSRN proteins in peritoneal macrophages, and found that only IFNγ lowered APOE and MFGE8 (Figure 3B). IFNγ also lowered both
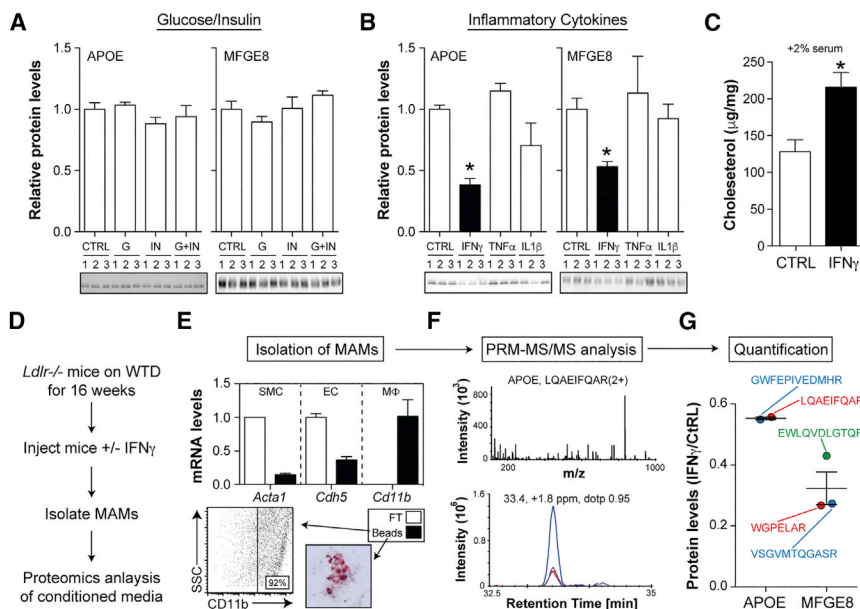
Figure 3. IFNγ Targets MSRN Proteins and Promotes Macrophage Cholesterol Accumulation

(A and B) APOE and MFGE8 levels in peritoneal macrophages treated with (A) vehicle (ctrl), 300 mg/dL glucose (G) or 10 nM insulin (I), alone or in combination (G+I), or (B) 12 ng/mL IFNγ, tumor necrosis factor alpha (TNF-α), or interleukin-1β (IL-1β) for 24 hr.

(C) Cholesterol levels in control and IFNγ-treated macrophages exposed to 2% serum from WTD-fed *Ldlr−/−* mice.

(D) *Ldlr−/−* mice were fed a WTD for 16 weeks and injected with vehicle or IFNγ, and murine aortic macrophages (MAMs) were isolated.

(E) MAM purity was assessed by qRT-PCR for smooth muscle cells (SMC), endothelial cells (EC), and macrophage (Mφ) markers in anti-CD11b bound (beads) and unbound (FT) cells, flow cytometry, and Oil-red-O staining.

(F) Representative LC-MS/MS spectrum and ion chromatograms from parallel reaction monitoring.

(G) Relative quantification of APOE and MFGE8 for all peptides in IFNγ-injected versus control mice. Results are mean ± SEM.

*p < 0.05 (t test); n = 3–5 mice/group. See also Figures S3 and S4.

MSRN proteins in bone-marrow-derived macrophages and human monocyte-derived macrophages *in vitro* (Figure S3). Moreover, treatment with IFNγ, increased macrophage cholesterol levels following exposure to 2% serum from WTD-fed *Ldlr−/−* mice (Figure 3C).

To determine if IFNγ could alter MSRN proteins *in vivo*, we developed a mass spectrometry approach to interrogate murine aortic macrophages (MAMs) (Figure 3D). *Ldlr−/−* mice were fed a WTD for 16 weeks to allow MAMs to accumulate in the artery wall. At this time, mice were injected with IFNγ (IP, 25 μg/kg) or vehicle control; MAMs were purified (Figure 3E); and MSRN protein levels in the conditioned media were quantified by proteomics.

Because of the limited number of MAMs in mice, we first developed a selected reaction monitoring method (Hoofnagle et al., 2012) to quantify several MSRN proteins in small numbers of macrophages. After validating that this approach could reliably quantify APOE in 50,000 macrophages *in vitro* (Figure S4), we analyzed the abundance of APOE and MFGE8 in MAM-conditioned media *in vivo*. Results showed that IFNγ lowered both APOE and MFGE8 levels in MAMs *in vivo* (Figures 3F and 3G). Thus, IFNγ is capable of targeting MSRN proteins in murine artery wall macrophages.

IFNγ Induction during Obesity/IR Targets the MSRN without Inducing Host Defense Genes

Since IFNγ targeted MSRN proteins and enhanced cholesterol loading *in vitro*, we reasoned that it was required for obesity/IR to elicit similar effects *in vivo*. We first determined if IFNγ levels were raised in the "obesity/IR only" model. Because plasma IFNγ levels were undetectable, we quantified IFNγ production by splenic T cells and found that obesity/IR induced IFNγ (Figure 4A).

Next, we investigated whether blocking IFNγ signaling (by knocking out its receptor, *Ifngr1−/−*) normalized MSRN proteins and macrophage cholesterol accumulation in the "obesity/IR only" model. Deleting *Ifngr1* did not correct metabolic parameters in obese/IR mice (Figure 4B), a finding that, when combined with previous work (Rocha et al., 2008), suggests that IFNγ does not appreciably contribute to insulin resistance.

On the other hand, deleting *Ifngr1* blocked the ability of obesity/IR to alter MSRN proteins (Figure 4C; Table S1) and increased macrophage cholesterol accumulation following treatment with 2% serum from WTD-fed *Ldlr−/−* mice (Figure 4D). This lower cholesterol accumulation could not be explained by changes in *Abca1*, *Abcg1*, *Lxra*, *Cd36*, *Sra1*, or *Srebp2*, all of which were unaffected by *Ifngr1* deletion (Figure 4E).

Although these data support a model wherein IFNγ alters MSRN proteins which, in turn, predisposes macrophages to excessive cholesterol accumulation, IFNγ also alters hundreds of host defense genes (Shtrichman and Samuel, 2001) that could potentially explain this effect. Surprisingly, obesity/IR did not induce IFNγ-target genes (*Irf1*, *Irf8*, and *Ibp1*) or phosphorylation of STAT1 (required for target gene induction) in macrophages from WT C57BL/6 mice, nor were IFNγ-target genes lowered when *Ifngr1* was deleted (Figures 4F and 4G). Thus, the effects of IFNγ on the MSRN during obesity/IR are specific.

IFNGR1 is essential for IFNγ signaling, and we confirmed that IFNγ could not target MSRN proteins or host defense genes in *Ifngr1−/−* macrophages *in vitro* (Figure S5). How could blocking IFNγ signaling *in vivo* normalize MSRN proteins without altering known IFNγ-target genes or signaling? Much of our understanding of how IFNγ affects macrophages is based on doses (∼10 ng/mL) that are much higher than those in patients with T2D (∼50 pg/mL) (Mirhafez et al., 2015; Nosratabadi et al., 2009) or those produced by T cells in obese/IR mice (see Figure 4A).
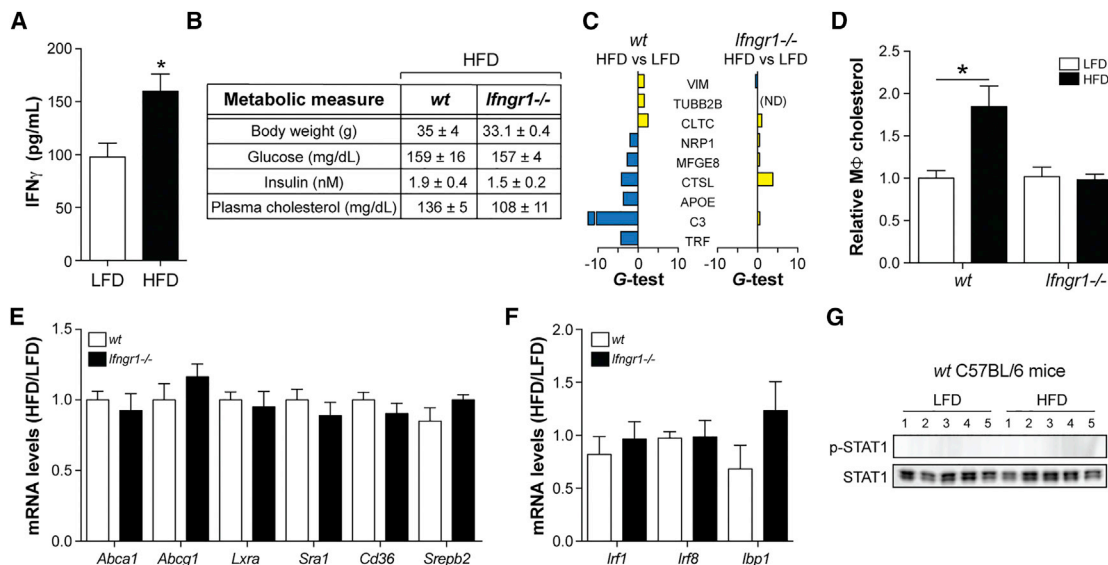
Figure 4. Deleting *Ifngr1* Corrects MSRN Proteins and Macrophage Cholesterol Levels in the "Obesity/IR Only" Model

(A–G) WT and *Ifngr1*−/− mice were fed a LFD or HFD for 9 weeks.

(A) IFNγ production by splenic T cells in WT mice.

(B) Metabolic parameters.

(C–F) Peritoneal macrophage MSRN protein levels (C), cholesterol levels following treatment with 2% serum from WTD-fed *Ldlr*−/− mice (D), cholesterol metabolism gene levels (E), and IFNγ-target gene levels (F).

(G) p-STAT1/STAT1 levels.

Results are mean ± SEM. *p < 0.05 (t test); n = 4–10 mice/group. See also Table S1.

We reasoned that "metabolic disease appropriate" doses of IFNγ specifically target the MSRN. Consistent with this interpretation, lower IFNγ doses (30–120 pg/mL) suppressed APOE (Figure 5A), but did not induce STAT1 phosphorylation, *Irf8* expression, or macrophage bacterial killing, all of which required higher doses (1.2–12 ng/mL) (Figures 5B–5D).

Following ligand binding, IFNGR1 heterodimerizes with IFNGR2, resulting in phosphorylation and nuclear translocation of STAT1 to induce interferon regulatory factors (IRFs) that upregulate additional genes essential to host defense (Ikushima et al., 2013). Our demonstration that MSRN dysregulation and host defense pathways can be dissociated by altering IFNγ dose implies that distinct pathways (downstream of IFNGR1) control these diverse functional properties.

To begin to test this hypothesis, we investigated whether knocking down *Stat1* with small interfering RNA (siRNA), or knocking out *Irf1* (*Irf1*−/−), two key components of the host defense pathway, could block IFNγ's effect on the MSRN. We treated siRNA-control and siRNA-*Stat1* (~80% knockdown) (Figure 5E) or WT and *Irf1*−/− macrophages with 12 ng/mL IFNγ. Lowering STAT1 levels or knocking out IRF1 blocked the ability of IFNγ to induce bacterial killing by macrophages, but had no effect on its ability to suppress APOE (Figures 5F and 5G). These findings suggest that IFNγ might alter MSRN proteins through a mechanism that is independent of the canonical pathway required for host defense. Although this interpretation is consistent with our *in vivo* findings (see Figure 4), further experimentation will be required to delineate this putative mechanism.

Myeloid Cell Deletion of *Ifngr1* Attenuates Atherosclerosis in *Ldlr*−/− Mice Only when Obesity/IR Is Present

Our findings suggested that obesity/IR was required to induce IFNγ and its pro-atherogenic actions on macrophages. Furthermore, atherogenic effects of IFNγ are well supported in mouse studies (Ramji and Davies, 2015). Based on these findings, we hypothesized that obesity/IR induces IFNγ production, which, in turn, alters MSRN proteins to promote macrophage cholesterol accumulation and atherogenesis in the presence of hypercholesterolemia. This hypothesis makes several predictions.

First, IFNγ should be elevated in the "HC and obesity/IR" model, but not the "HC only" model. Indeed, we found that IFNγ production by splenic T cells was increased in *Ldlr*−/− mice fed the WTD, but not the HCLF diet (Figure 6A), and these IFNγ levels were similar to those observed in the "obesity/IR only" model (see Figure 4A).

Second, myeloid cell deletion of *Ifngr1* should normalize MSRN proteins in the "HC and obesity/IR" model, but not the "HC only" model. To test this, we created mice lacking *Ifngr1* in myeloid cells by transplanting *Ifngr1*−/− (or WT) bone marrow cells into *Ldlr*−/− mice (Figure S6), and fed them a chow diet, a WTD, or a HCLF diet. Deleting *Ifngr1* in myeloid cells did not correct metabolic parameters (Figure 6B), which mimicked our findings in the "obesity/IR only" model. In contrast, deleting *Ifngr1* in myeloid cells restored 5/9 MSRN proteins in WTD-fed *Ldlr*−/− mice, but had no effect on these proteins in HCLF diet-fed mice (Figures 6C and 6D; Table S1).
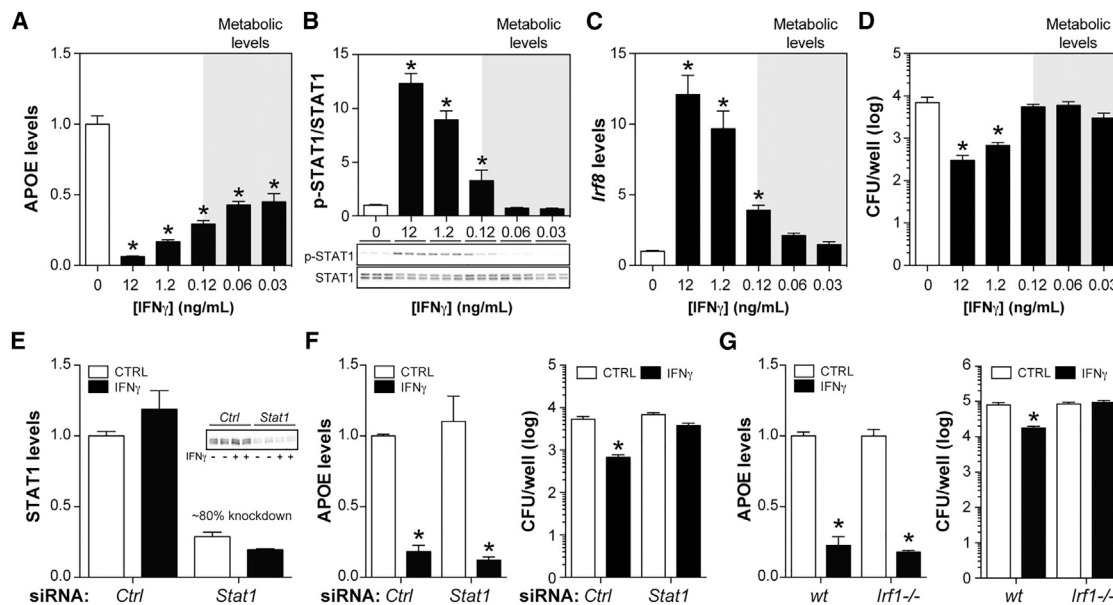
Figure 5. "Metabolic Disease Appropriate" Doses of IFNγ Specifically Target MSRN Proteins

(A–D) Macrophages were treated with varying levels of IFNγ.

(A) APOE levels.

(B) p-STAT1/STAT1 levels.

(C) *Irf8* levels.

(D) Number of *P. aeruginosa* remaining after incubation with macrophages.

(E) Efficiency of STAT1 knockdown in macrophages treated with control or *Stat1* siRNA. STAT1 levels were quantified 30 min after IFNγ exposure.

(F and G) Effects of IFNγ on APOE levels and number of *P. aeruginosa* remaining after incubation with siRNA control or siRNA *Stat1* macrophages (F) and WT or *Irf1*−/− macrophages (G).

Results are mean ± SEM. *p < 0.05 (t test); n = 3–10 biological replicates/group. See also Figure S5.

Third, correction of MSRN proteins in myeloid cell *Ifngr1*−/− mice should be specific. Similar to the "obesity/IR only model," IFNγ-target genes and STAT1 phosphorylation were not elevated in *Ldlr*−/− mice fed the WTD or HCLF diet (Figures 6E and 6F), and IFNγ-target genes were not lowered when *Ifngr1* was deleted from myeloid cells (Figure 6G).

Fourth, myeloid cell deletion of *Ifngr1* should attenuate macrophage cholesterol accumulation in the "HC and obesity/IR" model, but not the "HC only" model. Deleting *Ifngr1* in myeloid cells lowered macrophage cholesterol levels in WTD-fed *Ldlr*−/− mice, but not in HCLF-diet-fed mice (Figure 6H). The reduced foam cell formation in WTD-fed mice could not be explained by changes in *Abca1*, *Abcg1*, *Lxra*, *Cd36*, *Sra1*, or *Srebp2*, all of which were unaffected in *Ifngr1*-deficient macrophages (Figure 6I).

Fifth, this hypothesis predicts that myeloid cell deletion of *Ifngr1* should lessen atherosclerotic lesion size in the "HC and obesity/IR" model, but not the "HC only" model. Deleting *Ifngr1* in myeloid cells reduced aortic root lesion area in *Ldlr*−/− mice fed the WTD for 12 weeks (Figures 6J and S6), and this reduction could not be explained by changes in metabolic parameters (see Figure 6B) or plasma lipoprotein distribution (Figure S6). In contrast, lesion area was not lowered in mice fed the HCLF diet for 15 weeks (to compensate for delayed lesion formation) (Figures 6J and S6).

Finally, this hypothesis predicts that blocking IFNγ action on macrophages should abolish the relationship between obesity/

IR and atherosclerosis (Gruen et al., 2006). As shown in Figures 6K and 6L, plasma insulin levels, but not plasma cholesterol levels, were positively correlated to aortic root lesion size in WTD-fed *Ldlr*−/− mice. This relationship was abolished in mice transplanted with *Ifngr1*−/− cells (Figures 6K and 6L), even though metabolic parameters were not corrected (see Figure 6B).

DISCUSSION

Compared to non-diabetics, patients with T2D have a 4-fold increased risk for cardiovascular disease, which accounts for ∼70% of the morbidity in these patients (Gore et al., 2015; Haffner et al., 1998). Despite these staggering statistics, mechanisms explaining this risk are poorly understood, partly because diets that induce obesity/IR and T2D in *Ldlr*−/− and *Apoe*−/− mice fed a WTD, the most common murine models of atherosclerosis, also elevate plasma cholesterol levels. Thus, it has been challenging to ascertain direct effects of T2D, which is important because the increased cardiovascular events in these patients cannot be fully explained by hypercholesterolemia (Costa et al., 2006).

To overcome this problem, we used genetic (WT, *Ldlr*−/− mice) and dietary (HFD, WTD, HCLF diets) interventions to study macrophages from mice with obesity/IR only, HC and obesity/IR, and HC only. Using this approach, we identified an
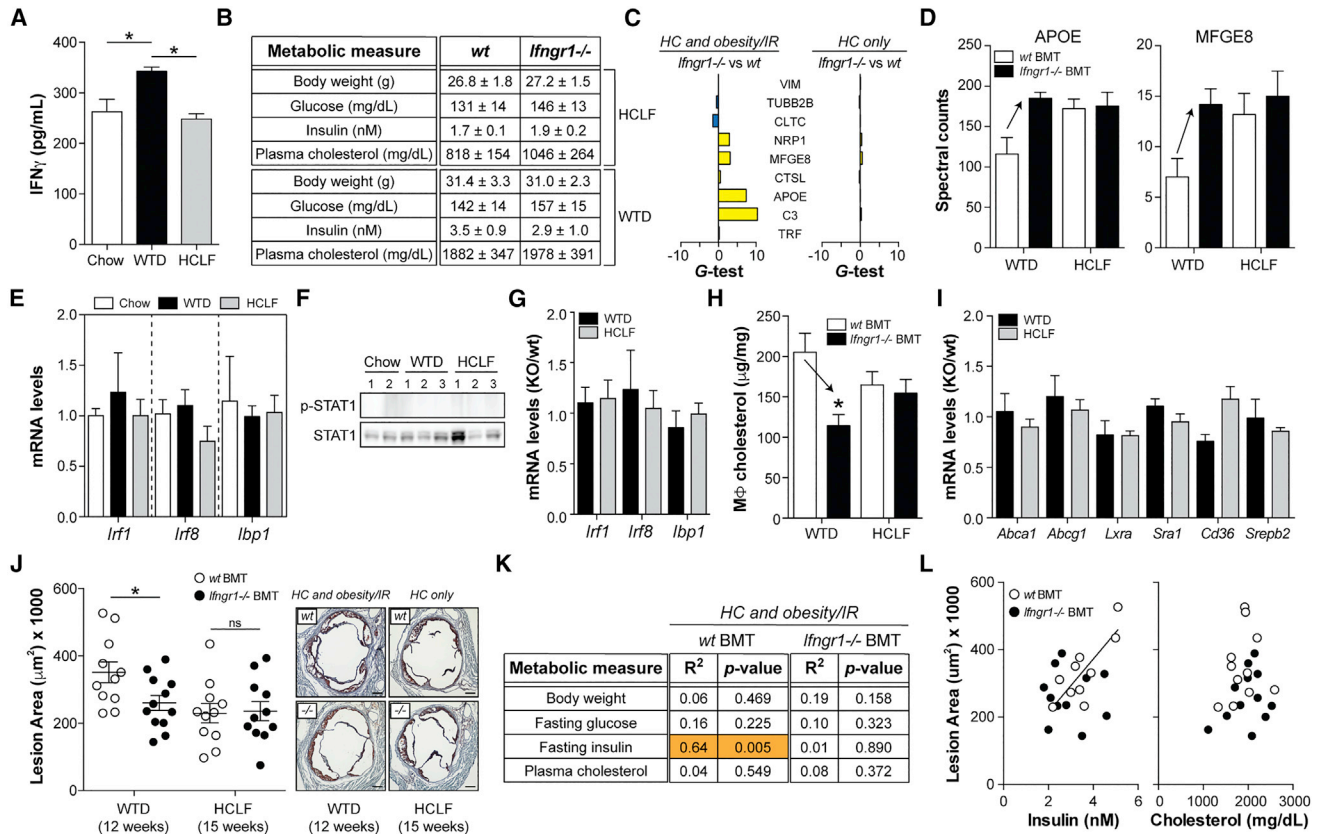
Figure 6. Macrophage IFNGR1 Is Required for Obesity/IR to Target MSRN Proteins, Increase Macrophage Cholesterol Accumulation, and Promote Atherosclerosis

(A–L) *Ldlr*−/− mice transplanted with WT or *Ifngr1*−/− bone marrow cells were fed a chow diet, a WTD, or a HCLF diet for up to 15 weeks.

(A) IFNγ production by splenic T cells in WT mice.

(B) Metabolic parameters.

(C–I) Peritoneal macrophage MSRN protein levels (C and D), IFNγ-target gene levels in WT mice (E), p-STAT1/STAT1 levels in WT mice (F), IFNγ-target gene levels in WT and *Ifngr1*−/− mice (G), cholesterol levels (H), and cholesterol metabolism gene levels (I).

(J) Aortic root lesion area and representative images. Scale bar, 200 μm.

(K) Relationships between metabolic parameters and aortic root lesion area.

(L) Relationships between fasting insulin or plasma cholesterol levels and aortic root lesion area.

Results are mean ± SEM. *$p < 0.05$ (t test); n = 3–12 mice/group. See also Figure S6 and Table S1.

IFNγ-macrophage-MSRN pathway that promotes foam cell formation and atherogenesis, only in the context of obesity/IR.

Three lines of evidence support the specificity of this pathway for obesity/IR. First, we demonstrated that obesity/IR is both necessary and sufficient to induce IFNγ production by T cells. Second, blocking IFNγ signaling in macrophages (by *Ifngr1*−/− bone marrow transplantation) attenuated atherosclerosis in *Ldlr*−/− mice with obesity/IR, but did not affect lesion size in *Ldlr*−/− mice without obesity/IR. Third, blocking IFNγ signaling in macrophages abolished the strong relationship between hyperinsulinemia and aortic root lesion size, even though the extent of obesity/IR was unaffected in the mice.

These findings suggest that some of the mechanisms regulating atherosclerosis in the presence and absence of obesity/IR are distinct and identify IFNγ as a T2D-specific driver of atherogenesis. Therapies targeting pro-inflammatory cytokines in patients with increased risk of cardiovascular disease are un-

derway (Ridker, 2016). In addition to these efforts, our work suggests that anti-IFNγ therapeutics might be particularly beneficial for lowering risk in patients with T2D.

On a molecular level, we showed that IFNγ suppressed specific anti-atherogenic MSRN proteins (i.e., APOE and C3), which predispose macrophages to increased cholesterol accumulation. Macrophages from obese/IR mice had reduced APOE and C3 levels, but did not exhibit deficits in other cholesterol metabolism genes, including *Abca1*, *Abcg1*, *Cd36*, *Lxra*, *Sra1*, and *Srepb2*. Similarly, ablating *Ifngr1* attenuated foam cell formation and restored APOE and C3 levels, but had no effect on the cholesterol metabolism genes. Thus, the suppression of APOE and C3, and perhaps other MSRN proteins, represents a key mechanism by which IFNγ and obesity/IR promote foam cell formation.

IFNγ-induced changes to MSRN proteins are insufficient to cause foam cell formation (or atherogenesis) in the absence of

hypercholesterolemia. Instead, they create a molecular susceptibility that, in the presence of hypercholesterolemia, increases macrophage cholesterol accumulation, a central event in atherogenesis. From this perspective, obesity/IR can be conceptualized as a perturbation that "sensitizes macrophages to atherogenic lipoproteins," which may help to explain why type 2 diabetics generally require more aggressive cholesterol lowering to achieve therapeutic benefit (Banach et al., 2016; Hoe and Hegele, 2015).

Importantly, deleting *Ifngr1* did not affect metabolic parameters in normocholesterolemic (WT) or hypercholesterolemic (*Ldlr*−/−) mice, which agrees with previous studies using *Ifng*−/− mice (Rocha et al., 2008). The uncoupling of the metabolic and pro-atherogenic functions of IFNγ might help to explain the curious relationship between metabolic dysfunction and atherosclerotic risk in patients with T2D. While elevated HBA1c levels are an excellent predictor of atherosclerotic risk, therapeutically lowering HBA1c does not necessarily alleviate this risk (Hayward et al., 2015). These data suggest that T2D induces factor(s) that promote atherogenesis, but that these factor(s) are not necessarily corrected by insulin sensitizing interventions. Recent studies showed that systemic and adipose tissue inflammation persists following bariatric surgery despite correction of hyperglycemia and insulin sensitivity (Kratz et al., 2016). Based on these observations and our work, we speculate that IFNγ might be one of these factors; however, additional studies will be needed to confirm this hypothesis.

IFNγ-producing immune cells are prominent in human and murine atheromas (Libby et al., 2013), and atherogenic effects of IFNγ are well supported in mouse studies (Ramji and Davies, 2015). However, the dietary conditions supporting its induction, the molecular changes it induces *in vivo*, and the cellular target(s) that mediates its pro-atherogenic effects are incompletely understood.

We showed that the induction of IFNγ requires the presence of obesity/IR. Surprisingly, the IFNγ levels produced during obesity/IR specifically targeted macrophage MSRN proteins, without inducing canonical signaling through STAT1 or its target genes involved in host defense. The latter required IFNγ doses several orders of magnitude higher than those observed in obese/IR mice or patients with T2D. Similarly, ablating *Ifngr1* (the ligand binding receptor) corrected MSRN proteins and attenuated foam cell formation and atherosclerosis, but did not affect established IFNγ-target genes.

These findings suggest that the pro-atherogenic actions of IFNγ on macrophages may be independent of its canonical signaling pathway, which is supported by previous studies showing that myeloid cell deletion of *Stat1* or *Ifngr2*, two key components of this signaling pathway (Ikushima et al., 2013), failed to attenuate atherogenesis (Boshuizen et al., 2016; Lim et al., 2008). Consistent with this hypothesis, previous studies showed that IFNγ alters expression of many genes in *Stat1*−/− macrophages (Gil et al., 2001), suggesting that STAT1-independent mechanisms significantly contribute to the effects of this cytokine on macrophage gene expression and function.

Future studies aimed at delineating this putative host-defense-independent mechanism and its contribution to atherosclerosis and infection models may inform therapeutic approaches to target IFNγ biology to treat cardiovascular disease in patients with T2D without predisposing them to opportunistic infections.

EXPERIMENTAL PROCEDURES

Mice

All animal studies were approved by the University of Chicago IACUC (ACUP#72209) and performed in accordance with the NIH Guide for the Care and Use of Laboratory Animals. WT (CD45.1 or CD45.2), *Ldlr*−/−, *Irf1*−/−, and *Ifngr1*−/− mice on the C57BL/6 background came from Jackson Labs. For diet-induced obesity (DIO) studies, WT and *Ifgnr1*−/− male mice (8 weeks of age) were placed on an LFD (20:50503, PicoLab) or 60% HFD (D12492, Research Diets) for 9 weeks. For atherosclerosis studies, *Ldlr*−/− mice (8 weeks of age) or chimeric mice (6 weeks post-transplantation) were placed on an LFD (20:50503, PicoLab), low-fat high cholesterol (Envigo TD02026), or Western-type diet (TD96121, Harlan Teklad) for up to 16 weeks.

Blood Measurements

Serum insulin levels were measured by ELISA (Millipore), and blood glucose levels were measured with a One Touch Ultra 2 glucometer (Lifescan) following a 3-hr fast. Total plasma cholesterol levels and cholesterol levels within the very low density lipoprotein (VLDL), LDL, and HDL fractions were obtained by an Amplex Red Cholesterol Assay Kit (Invitrogen). Lipoproteins were separated by fast protein liquid chromatography on two Superose 6 size-exclusion columns in tandem (GE Lifescience).

Bone Marrow Transplantation

Bone marrow cells (5×10^6) collected by PBS perfusion of the femurs and tibia of 8-week-old *Ifngr1*−/− or WT (CD45.1) male mice were injected into the retro-orbital sinus of lethally irradiated (9.5 Gy ionizing radiation) 8-week-old male *Ldlr*−/− recipient mice. Mice were maintained on a Uniprim diet for 1 week before and 2 weeks after transplant and allowed to recover for 6 weeks before initiation of diets. For WT transplants, engraftment was determined by flow cytometry using the ratio of CD45.1-positive (donor) to CD45.2-positive (recipient) bone marrow cells. For *Ifngr1*−/− transplants, engraftment was quantified by PCR as the ratio of *Ifngr1*−/− (donor) to WT (recipient) signal. See also Figure S6 and Table S2.

Quantification of Atherosclerosis

Anesthetized mice were perfused with PBS followed by 4% paraformaldehyde with 5% sucrose in PBS. The heart and upper vasculature were excised, cleaned of adventitia, and imbedded in optimal cutting temperature (OCT), and serial 10-μm sections in the aortic root were collected. Sections, beginning at the appearance of the coronary artery and aortic valve leaflets, were stained with Oil Red O/Fast green, and digital images were captured using a Nikon Eclipse Ti2 microscope. Aortic root lesion area was quantified by cross-sectional analysis of four sections/mouse (spaced 100 μm apart) using NIS Elements AR software.

Isolation and Analysis of BMDMs and Elicited Peritoneal Macrophages

Bone-marrow-derived macrophages (BMDMs) were prepared by culturing bone marrow cells in 30% L cell-conditioned media for 7 days (Kratz et al., 2014). Elicited peritoneal macrophages were isolated by lavaging the peritoneal cavity with PBS containing 2% BSA (endotoxin-free) 5 days after 4% thioglycolate injection (3 mL/mouse) (Becker et al., 2010). Cells were plated in serum-free DMEM for 2 hr, washed with PBS, and cultured in DMEM with 10% fetal calf serum (FCS) for 24 hr prior to use. Macrophage-conditioned media were prepared by treating cells with glucose and/or insulin or cytokines for 24 hr, washing cells with PBS, and incubating them in serum-free media for an additional 24 hr. MSRN proteins in the macrophage-conditioned media were quantified by immunoblotting.

Isolation and Analysis of Human Monocyte-Derived Macrophages

Human peripheral blood was obtained from healthy volunteers as approved by the University of Chicago Institutional Review committee (IRB16-0321) and

following obtaining written consent. Monocytes were isolated using anti-CD14 coupled magnetic beads and differentiated into human monocyte-derived macrophages by treating with M-CSF for 7 days as previously described (Kratz et al., 2014). Cells were treated for 24 h with vehicle or IFNγ, and effects on media APOE levels were determined by immunoblotting.

Isolation and Analysis of Murine Aortic Macrophages

Aortic macrophages were isolated from *Ldlr*−/− mice fed a Western diet for 16 weeks. Mice were injected intraperitoneally (i.p.) with PBS or IFNγ (25 μg/kg = 100 U/kg) (Whitman et al., 2000) 48 hr and 24 hr prior to euthanasia. Anesthetized mice were perfused with cold PBS with 20 U/mL heparin, and the upper vasculature was isolated and dissected of adipose tissue and para-aortic lymph nodes. The intima in the arch and innominate artery were excised and incubated in digestion media containing collagenase, hyaluronidase, and DNase1 in Hank's balanced salt solution (HBSS) for 1 hr (Butcher et al., 2011). Macrophages were isolated using anti-CD11b microbeads (Miltenyl Biotek) and plated in a 96-well dish in serum-free DMEM for 24 hr. Macrophage purity was assessed by flow cytometry on a Cantos II (BD Biosciences) and analyzed by FlowJo software (v.10.4.1).

Macrophage Cholesterol Loading

Macrophages were incubated for 24 hr in serum-free medium supplemented with or without 2% serum from *Ldlr*−/− mice fed a WTD for 12 weeks. Cellular lipids were extracted using isopropanol, dried, and solubilized in methanol: chloroform (2:1), and proteins were solubilized with 0.1% NaOH. Cholesterol levels were quantified using an Amplex Red Cholesterol Assay Kit (Invitrogen) and normalized to total cellular protein, which was measured using a Pierce BCA.

Macrophage siRNA Treatment

Macrophages were transfected with control siRNA or *Stat1* siRNA (Silencer Select, Ambion) using Lipofectamine RNAiMax (Invitrogen) and analyzed 48 hr post-transfection as previously described (Becker et al., 2010). STAT1 knockdown was confirmed by immunoblotting.

Macrophage Bacterial Killing

Macrophages were incubated with *P. aeruginosa* for 2 hr to allow for phagocytosis, treated with gentamicin to kill non-internalized bacteria, incubated for various times, and lysed, and live bacteria were plated on agar to quantify the number of colony-forming units (Hilbi et al., 2001).

Shotgun Proteomics

Conditioned media from 100,000 macrophages were diluted 1:1 with 1% sodium deoxycholate in 100 mM ammonium bicarbonate. Samples were denatured, reduced with 5 mM DTT by heating at 65°C for 1 hr, and alkylated with 15 mM iodoacetamide; excess iodoacetamide was quenched with additional 5 mM DTT; and samples were digested with trypsin (Promega, Madison, WI, USA) at a 1:20 w/w ratio overnight at 37°C. Samples were precipitated with 1% trifluoroacetic acid (TFA), desalted by solid phase extraction, dried down, and reconstituted with 0.1% formic acid in 5% acetonitrile. Digested peptides were injected on a trap column (40 × 0.1 mm, Reprosil C18, 5 μm, Dr. Maisch, Germany), desalted, and separated on a pulled-tip analytical column (400 × 0.075 mm, Reprosil C18, 5 μm, Dr. Maisch, Germany) heated to 50°C with a 3-segment linear gradient of acetonitrile, 0.1% FA in acetonitrile (Solution B), and 0.1% FA in water (Solution A) as follows: 0–2 min 1%–5% Solution B, 2–150 min 5%–25% Solution B, and 150–180 min 25%–35% Solution B (Waters NanoACQUITY).

Liquid chromatography-tandem mass spectrometry (LC-MS/MS) was acquired on Orbitrap Fusion Lumos (Thermo Scientific) operated in a data-dependent mode on charge states 2–4 with a 2-s cycle time, dynamic exclusion for 30 s, higher-energy collisional dissociation (HCD) fragmentation (normalized collision energy [NCE] 30%) and LC-MS/MS acquisition in the Orbitrap. MS spectra were acquired at resolution 120,000, and LC-MS/MS spectra (precursor selection window 1.6 Da) were acquired at a resolution of 30,000. Peptides and proteins were identified using the Comet search engine (Eng et al., 2015), with PeptideProphet and ProteinProphet validation (search criteria included a 20-ppm tolerance window for precursors and products and

Cys alkylation and methionine oxidation as fixed and variable modifications, respectively). Proteins considered for analysis had to be identified in at least 4 of 5 biological replicates for one dietary condition.

Targeted Proteomics

Proteins of interest were quantified using liquid chromatography Parallel Reaction Monitoring (PRM) MS on a Thermo Orbitrap Fusion Lumos tribrid mass spectrometer (Themo Scientific) connected to a NanoACQUITY HPLC (Waters). Several peptides from each proteins of interest were monitored by selecting their precursor ions in the quadrupole analyzer (selection window 1.6 Da) and full scan LC-MS/MS after HCD fragmentation (NCE 29%) in the Orbitrap analyzer with high resolution (15,000). Data were processed using Skyline software (MacLean et al., 2010). Identity of the chromatographic peaks was ascertained by matching the PRM LC-MS/MS spectrum to the spectra from the shotgun experiment (dot product > 0.9 and mass precision < 5 ppm). See also Figure S4.

IFNγ Production by T Cells

Isolated splenocytes (0.5×10^6 cells) were treated with anti-CD3 and anti-CD28 antibodies (eBioscience/Invitrogen) to activate T cells. After 48 hr, IFNγ levels in the media were measured using a Mouse IFNγ Ready-Set-Go ELISA Kit (eBioscience/Invitrogen).

Antibodies for Flow and Immunoblotting

The following were used for flow cytometry: anti-CD45.1, anti-CD45.2, anti-CD11b, anti-F4/80, and anti-CD11c (eBioscience/Invitrogen). The following were used for immunoblotting: rabbit anti-APOE (Abcam); goat anti-MFGE8 (R&D Systems); and rabbit anti-STAT1, rabbit anti-P-STAT1 (701), and rabbit anti-GAPDH (Cell Signaling).

qRT-PCR

RNA was isolated using QIAGEN Midi-Prep Kits and RT with Quantiscript (QIAGEN) using random hexamers (Invitrogen). mRNA levels were measured with specific primers (Table S2) using SYBR green on a One Step Plus system (Applied Biosystems). Relative levels of each target gene were calculated using the ΔΔCt formula and 18S RNA as a control.

Statistics

For proteomics studies, differentially expressed proteins were identified using a combination of the unpaired two-tailed Student's t test ($p < 0.05$) and G-test ($G > 1.5$) with correction for false discovery (FDR < 5%) as previously described (Heinecke et al., 2010). For all other studies, statistical significance ($p < 0.05$) was determined by an unpaired two-tailed Student's t test using Prism GraphPad software (v.6.0h). Data are presented as means ± SEM.

SUPPLEMENTAL INFORMATION

Supplemental Information includes six figures and two tables and can be found with this article online at https://doi.org/10.1016/j.celrep.2018.05.010.

AUTHOR CONTRIBUTIONS

Conceived and designed the experiments: all authors. Performed the experiments: C.A.R., A.L., K.Q.S., G.Z., C.C., H.J.-E., D.C., I.B., T.V., and A.H. Critically reviewed the manuscript: all authors. Wrote the manuscript: L.B. and C.A.R.

DECLARATION OF INTERESTS

The authors declare no competing interests.

REFERENCES

Banach, M., Nikolic, D., Rizzo, M., and Toth, P.P. (2016). IMPROVE-IT: what have we learned? Curr. Opin. Cardiol. 31, 426–433.

Barbu, A., Hamad, O.A., Lind, L., Ekdahl, K.N., and Nilsson, B. (2015). The role of complement factor C3 in lipid metabolism. Mol. Immunol. 67, 101–107.

Basu, S.K., Brown, M.S., Ho, Y.K., Havel, R.J., and Goldstein, J.L. (1981). Mouse macrophages synthesize and secrete a protein resembling apolipoprotein E. Proc. Natl. Acad. Sci. USA 78, 7545–7549.

Becker, L., Gharib, S.A., Irwin, A.D., Wijsman, E., Vaisar, T., Oram, J.F., and Heinecke, J.W. (2010). A macrophage sterol-responsive network linked to atherogenesis. Cell Metab. 11, 125–135.

Beckman, J.A., Creager, M.A., and Libby, P. (2002). Diabetes and atherosclerosis: epidemiology, pathophysiology, and management. JAMA 287, 2570–2581.

Boshuizen, M.C., Neele, A.E., Gijbels, M.J., van der Velden, S., Hoeksema, M.A., Forman, R.A., Muller, W., Van den Bossche, J., and de Winther, M.P. (2016). Myeloid interferon-γ receptor deficiency does not affect atherosclerosis in LDLR(-/-) mice. Atherosclerosis 246, 325–333.

Butcher, M.J., Herre, M., Ley, K., and Galkina, E. (2011). Flow cytometry analysis of immune cells within murine aortas. J. Vis. Exp. 53, 2848.

Chawla, A., Nguyen, K.D., and Goh, Y.P. (2011). Macrophage-mediated inflammation in metabolic disease. Nat. Rev. Immunol. 11, 738–749.

Costa, J., Borges, M., David, C., and Vaz Carneiro, A. (2006). Efficacy of lipid lowering drug treatment for diabetic and non-diabetic patients: meta-analysis of randomised controlled trials. BMJ 332, 1115–1124.

Donath, M.Y., and Shoelson, S.E. (2011). Type 2 diabetes as an inflammatory disease. Nat. Rev. Immunol. 11, 98–107.

Eng, J.K., Hoopmann, M.R., Jahan, T.A., Egertson, J.D., Noble, W.S., and MacCoss, M.J. (2015). A deeper look into Comet–implementation and features. J. Am. Soc. Mass Spectrom. 26, 1865–1874.

Fazio, S., Babaev, V.R., Burleigh, M.E., Major, A.S., Hasty, A.H., and Linton, M.F. (2002). Physiological expression of macrophage apoE in the artery wall reduces atherosclerosis in severely hyperlipidemic mice. J. Lipid Res. 43, 1602–1609.

Gil, M.P., Bohn, E., O'Guin, A.K., Ramana, C.V., Levine, B., Stark, G.R., Virgin, H.W., and Schreiber, R.D. (2001). Biologic consequences of Stat1-independent IFN signaling. Proc. Natl. Acad. Sci. USA 98, 6680–6685.

Gore, M.O., McGuire, D.K., Lingvay, I., and Rosenstock, J. (2015). Predicting cardiovascular risk in type 2 diabetes: the heterogeneity challenges. Curr. Cardiol. Rep. 17, 607.

Gruen, M.L., Saraswathi, V., Nuotio-Antar, A.M., Plummer, M.R., Coenen, K.R., and Hasty, A.H. (2006). Plasma insulin levels predict atherosclerotic lesion burden in obese hyperlipidemic mice. Atherosclerosis 186, 54–64.

Haffner, S.M., Lehto, S., Rönnemaa, T., Pyörälä, K., and Laakso, M. (1998). Mortality from coronary heart disease in subjects with type 2 diabetes and in nondiabetic subjects with and without prior myocardial infarction. N. Engl. J. Med. 339, 229–234.

Hartvigsen, K., Binder, C.J., Hansen, L.F., Rafia, A., Juliano, J., Hörkkö, S., Steinberg, D., Palinski, W., Witztum, J.L., and Li, A.C. (2007). A diet-induced hypercholesterolemic murine model to study atherogenesis without obesity and metabolic syndrome. Arterioscler. Thromb. Vasc. Biol. 27, 878–885.

Hayward, R.A., Reaven, P.D., and Emanuele, N.V.; VADT Investigators (2015). Follow-up of glycemic control and cardiovascular outcomes in type 2 diabetes. N. Engl. J. Med. 373, 978.

Heinecke, N.L., Pratt, B.S., Vaisar, T., and Becker, L. (2010). PepC: proteomics software for identifying differentially expressed proteins based on spectral counting. Bioinformatics 26, 1574–1575.

Hilbi, H., Segal, G., and Shuman, H.A. (2001). Icm/dot-dependent upregulation of phagocytosis by Legionella pneumophila. Mol. Microbiol. 42, 603–617.

Hoe, E., and Hegele, R.A. (2015). Lipid management in diabetes with a focus on emerging therapies. Can. J. Diabetes 39 (Suppl 5), S183–S190.

Hoofnagle, A.N., Becker, J.O., Oda, M.N., Cavigiolio, G., Mayer, P., and Vaisar, T. (2012). Multiple-reaction monitoring-mass spectrometric assays can accurately measure the relative protein abundance in complex mixtures. Clin. Chem. 58, 777–781.

Ikushima, H., Negishi, H., and Taniguchi, T. (2013). The IRF family transcription factors at the interface of innate and adaptive immune responses. Cold Spring Harb. Symp. Quant. Biol. 78, 105–116.

Kratz, M., Coats, B.R., Hisert, K.B., Hagman, D., Mutskov, V., Peris, E., Schoenfelt, K.Q., Kuzma, J.N., Larson, I., Billing, P.S., et al. (2014). Metabolic dysfunction drives a mechanistically distinct proinflammatory phenotype in adipose tissue macrophages. Cell Metab. 20, 614–625.

Kratz, M., Hagman, D.K., Kuzma, J.N., Foster-Schubert, K.E., Chan, C.P., Stewart, S., van Yserloo, B., Westbrook, E.O., Arterburn, D.E., Flum, D.R., and Cummings, D.E. (2016). Improvements in glycemic control after gastric bypass occur despite persistent adipose tissue inflammation. Obesity (Silver Spring) 24, 1438–1445.

Li, A.C., and Glass, C.K. (2002). The macrophage foam cell as a target for therapeutic intervention. Nat. Med. 8, 1235–1242.

Li, A.C., Binder, C.J., Gutierrez, A., Brown, K.K., Plotkin, C.R., Pattison, J.W., Valledor, A.F., Davis, R.A., Willson, T.M., Witztum, J.L., et al. (2004). Differential inhibition of macrophage foam-cell formation and atherosclerosis in mice by PPARalpha, beta/delta, and gamma. J. Clin. Invest. 114, 1564–1576.

Libby, P., Lichtman, A.H., and Hansson, G.K. (2013). Immune effector mechanisms implicated in atherosclerosis: from mice to humans. Immunity 38, 1092–1104.

Lim, W.S., Timmins, J.M., Seimon, T.A., Sadler, A., Kolodgie, F.D., Virmani, R., and Tabas, I. (2008). Signal transducer and activator of transcription-1 is critical for apoptosis in macrophages subjected to endoplasmic reticulum stress in vitro and in advanced atherosclerotic lesions in vivo. Circulation 117, 940–951.

MacLean, B., Tomazela, D.M., Shulman, N., Chambers, M., Finney, G.L., Frewen, B., Kern, R., Tabb, D.L., Liebler, D.C., and MacCoss, M.J. (2010). Skyline: an open source document editor for creating and analyzing targeted proteomics experiments. Bioinformatics 26, 966–968.

McNelis, J.C., and Olefsky, J.M. (2014). Macrophages, immunity, and metabolic disease. Immunity 41, 36–48.

Mirhafez, S.R., Pasdar, A., Avan, A., Esmaily, H., Moezzi, A., Mohebati, M., Meshkat, Z., Mehrad-Majd, H., Eslami, S., Rahimi, H.R., et al. (2015). Cytokine and growth factor profiling in patients with the metabolic syndrome. Br. J. Nutr. 113, 1911–1919.

Moore, K.J., Sheedy, F.J., and Fisher, E.A. (2013). Macrophages in atherosclerosis: a dynamic balance. Nat. Rev. Immunol. 13, 709–721.

Nosratabadi, R., Arababadi, M.K., Hassanshahi, G., Yaghini, N., Pooladvand, V., Shamsizadeh, A., Zarandi, E.R., and Hakimi, H. (2009). Evaluation of IFN-gamma serum level in nephropatic type 2 diabetic patients. Pak. J. Biol. Sci. 12, 746–749.

Ramji, D.P., and Davies, T.S. (2015). Cytokines in atherosclerosis: key players in all stages of disease and promising therapeutic targets. Cytokine Growth Factor Rev. 26, 673–685.

Ridker, P.M. (2016). From C-reactive protein to interleukin-6 to interleukin-1: moving upstream to identify novel targets for atheroprotection. Circ. Res. 118, 145–156.

Rocha, V.Z., Folco, E.J., Sukhova, G., Shimizu, K., Gotsman, I., Vernon, A.H., and Libby, P. (2008). Interferon-gamma, a Th1 cytokine, regulates fat inflammation: a role for adaptive immunity in obesity. Circ. Res. 103, 467–476.

Shtrichman, R., and Samuel, C.E. (2001). The role of gamma interferon in antimicrobial immunity. Curr. Opin. Microbiol. 4, 251–259.

Tabas, I., and Bornfeldt, K.E. (2016). Macrophage phenotype and function in different stages of atherosclerosis. Circ. Res. 118, 653–667.

Whitman, S.C., Ravisankar, P., Elam, H., and Daugherty, A. (2000). Exogenous interferon-gamma enhances atherosclerosis in apolipoprotein E-/- mice. Am. J. Pathol. 157, 1819–1824.

Supplemental Information

Obesity and Insulin Resistance Promote

Atherosclerosis through an IFNγ-Regulated

Macrophage Protein Network

Catherine A. Reardon, Amulya Lingaraju, Kelly Q. Schoenfelt, Guolin Zhou, Chang Cui, Hannah Jacobs-El, Ilona Babenko, Andrew Hoofnagle, Daniel Czyz, Howard Shuman, Tomas Vaisar, and Lev Becker
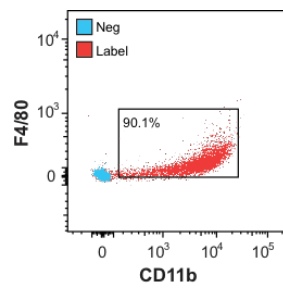
Fig. S1. Peritoneal macrophage purity (related to all figures). Wild-type or *Ifngr1-/-* C57BL6 mice or *Ldlr-/-* mice fed the various diets were injected with thioglycolate in the peritoneal cavity, and elicited peritoneal macrophages were isolated five days after injection. Peritoneal macrophage purity was confirmed by flow cytometry using antibodies raised against murine F4/80 and CD11b. A representative image is shown.
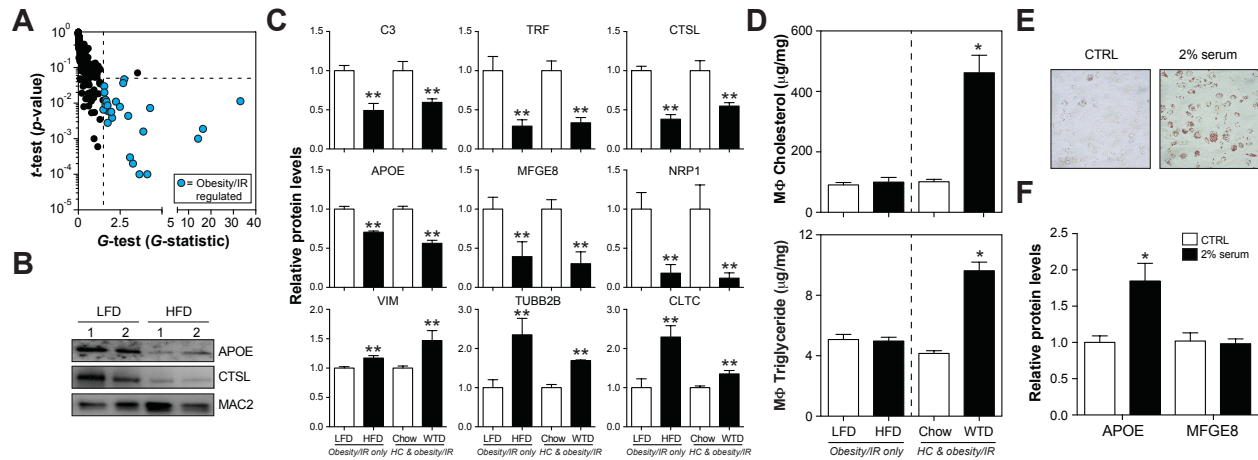
Fig. S2. Obesity/IR targets the MSRN, a pro-atherogenic macrophage protein network (related to Fig. 1). For the '*obesity/IR only*' model, *wt* C57BL/6 mice were fed a low-fat (LFD) or high-fat diet (HFD) for 9 weeks. For the '*HC & obesity/IR*' model, *Ldlr-/-* mice were fed a chow or western-type diet (WTD) for 12 weeks. *Panel A*: Proteomics analysis of elicited peritoneal macrophages in the *obesity/IR only* model. Differentially expressed proteins (blue circles) were identified based on the *G*-test (*G*>1.5) and *t*-test ($p<0.05$). *Panel B*: Immunoblotting validation for changes in protein abundance for APOE and CTSL. MAC2 was used as a control. *Panel C*: Regulation of the 9 MSRN proteins. *Panel D*: Peritoneal macrophages cholesterol and triglyceride levels. *Panels E-F*: Peritoneal macrophages were treated with and without 2% serum from WTD-fed *Ldlr-/-* mice. Cholesterol loading was confirmed by Oil-red-O staining (*Panel E*) and media APOE and MFGE8 were quantified (*Panel F*). Results show that *in vitro* cholesterol loading does not replicate the MSRN protein changes observed in WTD-fed *Ldlr-/-* mice. Results are mean ± SEM. *, $p<0.05$ (*t*-test). **, *G*>1.5 (*G*-test) and $p<0.05$ (*t*-test). n=2-5 mice/group.
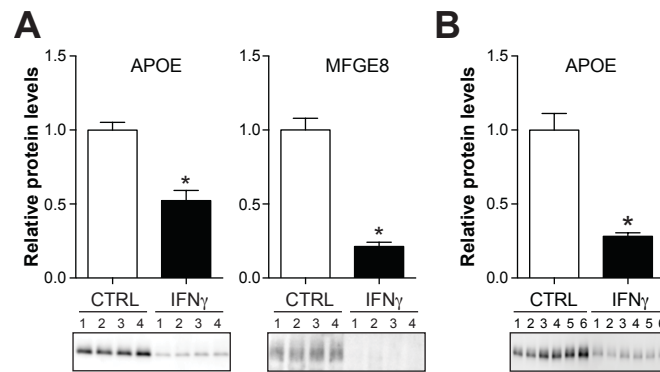
Fig. S3. IFNγ targets MSRN proteins in many types of macrophages (related to Fig. 3). APOE and/or MFGE8 protein levels in conditioned media collected from murine bone marrow-derived macrophages (*Panel A*) or human monocyte-derived macrophages (*Panel B*) treated with vehicle (CTRL) or IFNγ (12 ng/mL) for 24h. Results are mean ± SEM. *, *p*<0.05 Student's *t*-test. n=4-6 biological replicates/group.
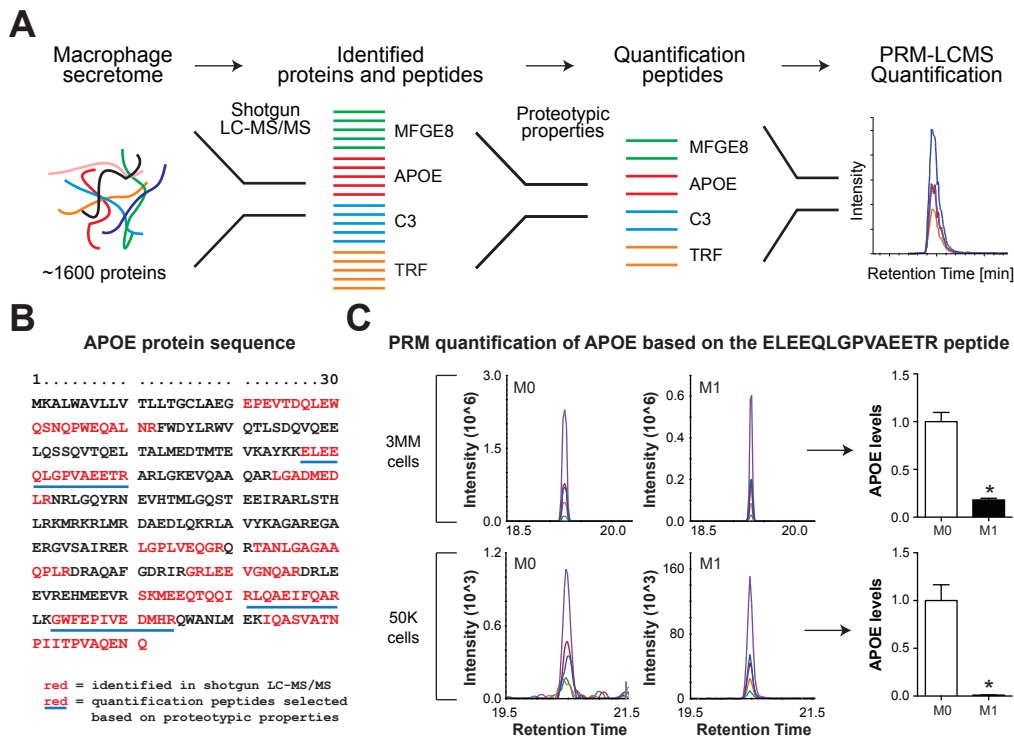
Fig. S4. A parallel reaction monitoring method for quantifying MSRN proteins in limited numbers of macrophages (related to Fig. 3). _Panel A_: Development of a targeted proteomics assay for quantification of MSRN proteins. MSRN proteins and identified peptides were selected from shotgun proteomics analysis and further evaluated for proteotypic properties using public resources. Best peptides (up to 5 per protein where available) were selected and further investigated using Parallel Reaction Monitoring LCMS in samples from unstimulated (M0) or classically activated (M1) BMDMs. Two conditioned were used: 3 million macrophages were cultured, proteins in the conditioned media were precipitated, and 0.2 μg was injected, or 50,000 macrophages were cultured and conditioned media were analyzed directly. _Panel A_: Workflow diagram. _Panel B_: Protein sequence of APOE indicating peptides selected for PRM quantification. _Panel C_: Quantification of APOE based on the ELEEQLGPVAEETR peptide in 3million or 50,000 M0 and M1 macrophages.

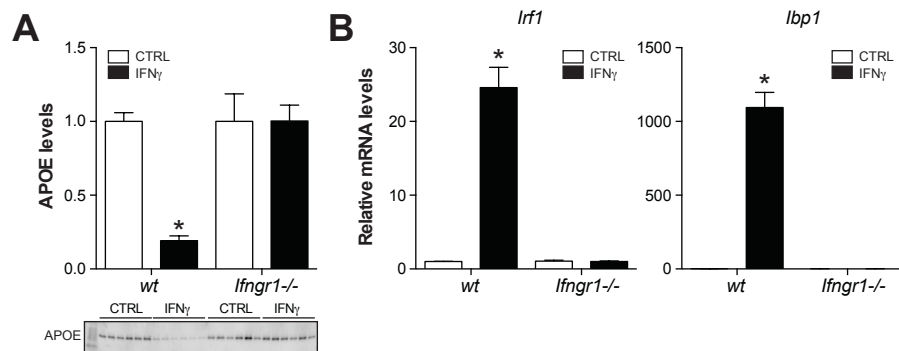**Fig. S5. IFNGR1 is required for IFNγ to target MSRN proteins and its target genes *in vitro* (related to Figs. 4-6).** Wild-type (*wt*) and *Ifngr1-/-* macrophages were treated with vehicle (CTRL) or 12ng/mL IFNγ. <u>Panel A</u>: Media APOE levels. <u>Panel B</u>: mRNA levels of IFNγ-target genes. Results are mean ± SEM. *, *p*<0.05 Student's *t*-test. n=6 biological replicates/group.
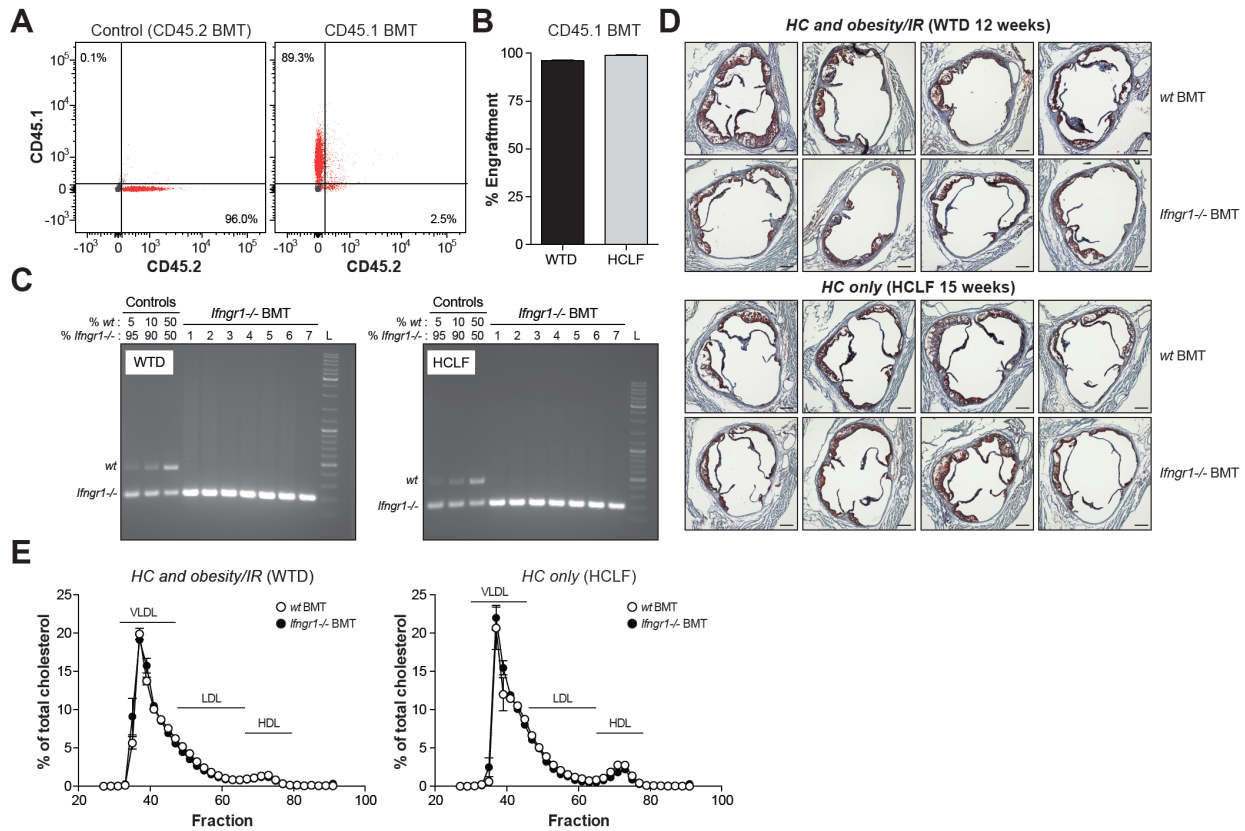
Fig. S6. Supplementary data for *wt* and *Ifngr1-/-* bone marrow transplants into *Ldlr-/-* mice (related to Fig. 6).
Ldlr-/- mice transplanted with *wt* or *Ifngr1-/-* bone marrow cells were fed a WTD or HCLF diet for up to 15 weeks.
<u>*Panels A-B*</u>: Engraftments for *wt* bone marrow transplants were assessed by flow cytometric analysis of the ratio of
CD45.1 (donor) to CD45.2 (recipient) positive bone marrow cells. <u>*Panel C*</u>: Engraftments for *Ifgnr1-/-* bone marrow
transplants were assessed by PCR analysis of the ratio of *Ifngr1-/-* (donor) and *wt* (recipient) in comparison to pre-
defined mixtures of bone marrow from *wt* and *Ifngr1-/-* mice. Seven mice per dietary condition are shown as
examples. All engraftments were judged to be >95%. <u>*Panel D*</u>: Cross-sections of the aortic root were stained with
Oil-red-O, counterstained with hematoxylin and fast green, and lesion area was quantified. Four representative
images are shown per group. Scale = 200 μm. <u>*Panel E*</u>: Plasma (100 μL) was fractionated by gel filtration using two
Superose-6 columns in tandem, and cholesterol levels in each fraction were quantified using the Amplex Red
Cholesterol Assay kit (Invitrogen). Results are mean ± SEM. n=5-12 mice/group.

	Obesity/IR only Model					
Protein annotations			**wt C57BL/6 mice HFD vs. LFD**		**Ifngr1-/- C57BL/6 mice HFD vs. LFD**	
Uniprot	**Entrez**	**Protein**	**G-test (HFD : LFD)**	**t-test**	**G-test (HFD : LFD)**	**t-test**
P01027	12266	C3	-16.43	0.0019	0.57	0.4722
Q921I1	22041	TRF	-4.30	0.0073	0.00	0.9792
P06797	13039	CTSL	-4.13	0.0001	3.80	0.0070
P08226	11816	APOE	-3.66	0.0001	0.00	0.9646
P21956	17304	MFGE8	-2.69	0.0368	0.49	0.1593
P97333	18186	NRP1	-2.02	0.0039	0.49	0.0509
P20152	22352	VIM	1.50	0.0066	-0.50	0.0820
B2RSN3	73710	TUBB2B	1.56	0.0201	ND	ND
Q68FD5	67300	CLTC	2.49	0.0079	1.04	0.0035

	HC +/- Obesity/IR Model					
Protein annotations			**Ldlr-/- mice WTD vs. Chow**		**Ldlr-/- mice HCLF vs. Chow**	
Uniprot	**Entrez**	**Protein**	**G-test (WTD : Chow)**	**t-test**	**G-test (HCLF : Chow)**	**t-test**
P01027	12266	C3	-9.80	0.0036	-0.01	0.8893
Q921I1	22041	TRF	-2.90	0.0082	0.31	0.2999
P06797	13039	CTSL	-4.46	0.0458	7.54	0.2722
P08226	11816	APOE	-12.72	0.0047	7.75	0.1559
P21956	17304	MFGE8	-3.03	0.0271	1.06	0.5212
P97333	18186	NRP1	-1.84	0.0013	0.85	0.4994
P20152	22352	VIM	3.57	0.0052	3.66	0.2052
B2RSN3	73710	TUBB2B	4.06	0.0169	0.78	0.4146
Q68FD5	67300	CLTC	2.63	0.0500	8.01	0.1054

	HC +/- Obesity/IR Model (Bone marrow transplantation)					
Protein annotations			**Ldlr-/- mice WTD (Ifngr1-/- vs. wt BMT)**		**Ldlr-/- mice HCLF (Ifngr1-/- vs. wt BMT)**	
Uniprot	**Entrez**	**Protein**	**G-test (-/- : wt)**	**t-test**	**G-test (-/- : wt)**	**t-test**
P01027	12266	C3	14.10	0.0190	0.29	0.6344
Q921I1	22041	TRF	0.19	0.1629	0.00	0.9837
P06797	13039	CTSL	0.50	0.1482	-0.25	0.1226
P08226	11816	APOE	7.37	0.0448	0.03	0.8749
P21956	17304	MFGE8	3.07	0.0073	0.52	0.2275
P97333	18186	NRP1	2.90	0.0030	0.38	0.1316
P20152	22352	VIM	0.00	0.9569	0.04	0.6143
B2RSN3	73710	TUBB2B	-0.52	0.0317	-0.24	0.1028
Q68FD5	67300	CLTC	-1.50	0.0240	0.02	0.6031

Table S1. Shotgun proteomics analysis of elicited peritoneal macrophages (related to Figs. 1, 4, 6). Proteomics analysis of the conditioned media collected from elicited peritoneal macrophages isolated from *wt* or *Ifngr1-/-* C57BL6 mice fed the LFD or HFD, from *Ldlr-/-* mice fed the chow, WTD, or HCLF diet, and from *Ldlr-/-* mice transplanted with *wt* or *Ifngr1-/-* bone marrow fed the WTD or HCLF diet. Proteomics data were analyzed by the G-test (G-statistic) and t-test (p-value). Differentially abundant proteins are shaded; red = up-regulated in 1st sample relative to the 2nd, green = down-regulated in the 1st sample relative to the 2nd. ND = not detected. n=3-5 mice/group.

Gene	Primer	Primer Sequence
Ifrngr1	Wild type	TCGCTTTCCAGCTGA
	Deficient	CTCGTGCTTTACGGTATCGC
	Common	CCACCTCAGCACTGTCTTCA
Srebp2	Forward	GTTGACCACGCTGAAGACAGA
	Reverse	CACCAGGGTTGGCACTTGAA
Abca1	Forward	GCTTGTTGGCCTCAGTTAAGG
	Reverse	GTAGCTCAGGCGTACAGAGAT
Sra1	Forward	TTCACTGGATGCAATCTCCAAG
	Reverse	CTGGACTTCTGCTGATACTTTG
Cd36	Forward	ATGGGCTGTGATCGGAACTG
	Reverse	GTCTTCCCAATAAGCATGTCTCC
Abcg1	Forward	GTGGATGAGGTTGAGACAGACC
	Reverse	CCTCGGGTACAGAGTAGGAAAG
Lxra	Forward	ACAGAGCTTCGTCCACAAAAG
	Reverse	GCGTGCTCCCTTGATGACA
Acta1	Forward	CCCAGACATCAGGGAGTAATGG
	Reverse	TCTATCGGATACTTCAGCGTCA
Cdh5	Forward	CCACTGCTTTGGGAGCCTT
	Reverse	GGCAGGTAGCATGTTGGGG
Cd11b	Forward	CCATGACCTTCCAAGAGAATGC
	Reverse	ACCGGCTTGTGCTGTAGTC
Irf1	Forward	GCTGGAGTTATGTCCCTTTCCATATC
	Reverse	GGACTCAGCAGCTCTACCCTACCT
Irf8	Forward	GCTGGTTCAGCTTTGTCTCC
	Reverse	GATCGAACAGATCGACAGCA
Ibp1	Forward	GTGTGGTAGAAGCCCACTATTGC
	Reverse	CCACATGAAAGGCCCAGTGTGC

Table S2. Primer Sequences for PCR (Related to Experimental Procedures).